An improved method for magnetic flux density visualization using three-dimensional edge finite element method

Vlatko Čingoski and Hideo Yamashita
Electric Machinery Laboratory, Hiroshima University, Higashi-hiroshima, 724 Japan

Visualization of a magnetic flux density distribution in three-dimensional (3-D) finite element analysis (FEA) is very important in order to grasp the real behavior of the magnetic field, especially in the design process. In this paper, we present an improved method for visualizing magnetic flux density distributions calculated by 3-D first-order edge FEA. Compared with traditional methods, this method provides more accurate, smoother magnetic flux density distribution inside the analyzed region and satisfies the proper boundary conditions across intermaterial boundaries. The usefulness of our algorithm is demonstrated with several examples.

I. INTRODUCTION

In the analysis of various magnetic field problems, analysts are usually interested in the values of magnetic flux density at certain points, or its distribution over part or all of the analyzed domain. Therefore, the visualization of such a distributed physical quantity is very important in order to grasp the real behavior of the magnetic field, and correctly understand and evaluate the results of analysis.

Recently, first-order edge based FEA has become a very popular for a wide class of 3-D magnetic field and eddy current problems. The main reasons are its computational efficiency, small memory requirements, and most of all satisfaction of only proper boundary conditions on the material interfaces.[1] Unfortunately, due to the discrete character of the magnetic flux density in each finite element, good visualization of the magnetic flux density obtained by first-order edge FEA is not possible.

In this paper, we proposed an improved visualization algorithm, which provides more accurate, smoother visualization of the results obtained from the 3-D edge FEA. The algorithm for the 2-D nodal FEA already presented in Ref. 2, here is extended into a third dimension and applied to the 3-D data obtained from the edge FEA. That is, the proposed algorithm is a mixed approach in the visualization process, successfully combining edge and nodal FEA over the same 3-D mesh. In order to demonstrate the validity of the proposed algorithm, two simple models, with and without magnetic materials, are presented.

II. OUTLINE OF THE ALGORITHM

In the traditional method, the magnetic flux density vector **B** can be obtained as

$$\mathbf{B} = \text{rot } \mathbf{A}, \tag{1}$$

in the finite number of lattice points inside the display space. Since we use a first-order edge finite elements, the values for **B** obtained from (1) are equal at any point inside the element. That is, discontinuous visualization of magnetic flux density vector **B** can be observed. To overcome this problem we developed the following algorithm.

(i) Using the magnetic vector potential data obtained by the 3-D edge FEA, from (1) we compute the magnetic flux density vector **B** previously at each vertex of the tetrahedron.

(ii) Since one vertex P of a tetrahedron usually belongs to more than one finite element, we compute the values of all three components of magnetic flux density vector **B** as an average value from all contributions of magnetic flux density at vertex P from all elements that have P as a vertex (Fig. 1). Therefore

$$B_{pj} = \frac{1}{n}\sum_{i=1}^{n} B_{pji} \tag{2}$$

where j is an x, y, or z component, and n is the total number of elements that have P as a vertex.

This procedure does not have a large influence on the values of magnetic flux density vector **B** obtained by (1) directly from the edge FEA, because if the mesh is suitably dense, the values at each vertex computed from adjacent elements differ to a small degree. It is necessary to perform this procedure only to provide a linear distribution of magnetic flux density vector **B** between any two points inside the element.

(iii) If vertex P is on the boundary between different magnetic materials, a new vertex P' is constructed, an infinitesimally small distance removed from P. The averaging procedure is performed for each material, and the calculated values are associated with P and P', respectively.

(iv) The magnetic flux density inside each finite element is approximated by the average values of each component of the magnetic flux density vector **B** at the four tetrahedron vertices. For approximation, we use some low-order interpolation formulas, such as shape functions, for first-order nodal analysis:

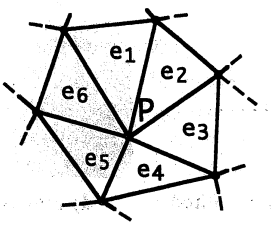

FIG. 1. Calculation of the magnetic flux density at vertex P.

 0021-8979/94/75(10)/6042/3/$6.00

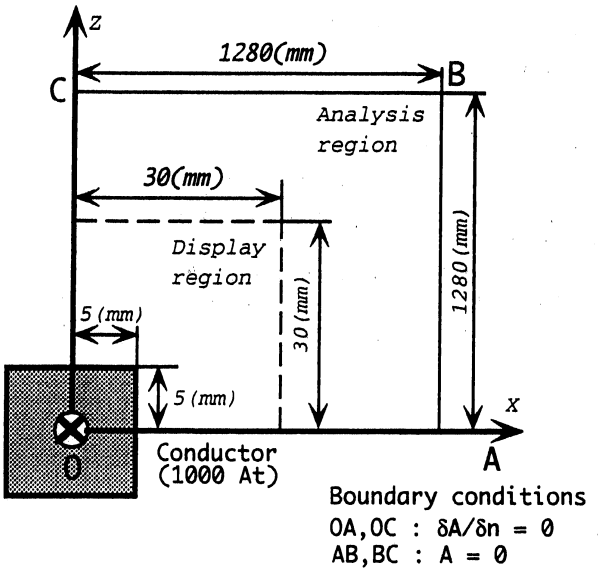

FIG. 2. Single-material model.

$$B_j = \sum_{i=1}^{4} N_i B_{ji}, \tag{3}$$

where j is the x, y, or z component of magnetic flux density. In this case, the distribution of magnetic flux density inside each finite element will be linear. Higher-order interpolation, e.g., quadratic, can be easily achieved using second-order

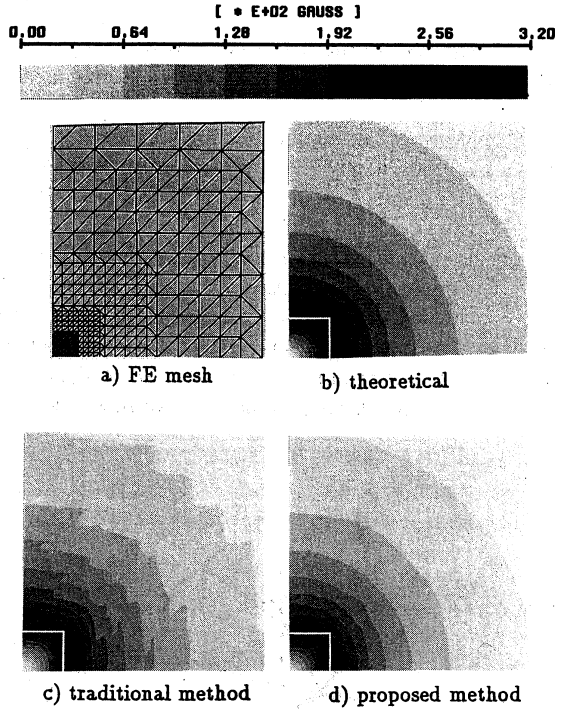

FIG. 3. Magnetic flux density distribution. (a) FE mesh, (b) theoretical (c) traditional method, and (d) proposed method.

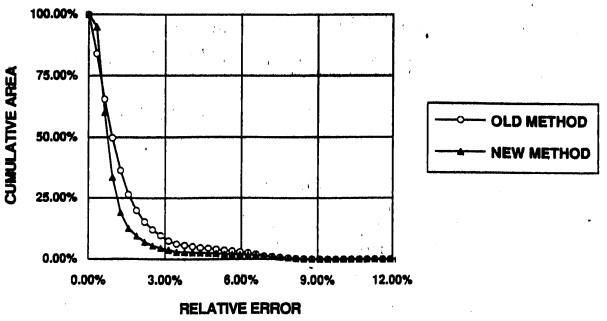

FIG. 4. Comparison of relative errors for traditional and proposed visualization methods.

nodal shape functions and six more values of magnetic flux density vector at midpoints of each edge of the element.

III. APPLICATION

In this section, we apply our method to the visualization of magnetic flux density for two models. One is a single-material model, of interest because of its known theoretical values, and the other is a multimaterial model, suitable for exploring the visualization on intermaterial boundaries.

A. Single-material region

Figure 2 shows the analysis and display region for the first model. Due to the symmetry of the model we performed analysis over only one quadrant. The calculated results are displayed in Fig. IV for theoretical, traditional, and our new visualization method using the same scale. Figure 3 also shows a division map used in the analysis. It is obvious that with no changing of the intensity of the magnetic flux density vector **B**, its distribution displayed by our method is almost identical with the theoretically obtained one, while the traditional visualization method results in a discontinuous distribution. In Fig. 4, the x axis represents relative error ϵ given as

$$\epsilon = \left| \frac{\mathbf{B}_t - \mathbf{B}_c}{\mathbf{B}_t} \right| \cdot 100, \tag{4}$$

where $\mathbf{B}_t$ and $\mathbf{B}_c$ are the theoretical and computed values for the magnetic flux density vector **B** at each lattice point inside the display space, respectively. In the same time, the y axis represents the cumulative area, given as

$$\text{cumulative area} = \frac{\text{display area with error over } \epsilon\ (\%)}{\text{total display area}} \cdot 100. \tag{5}$$

Figure 4 clearly shows that the relative error of the proposed method is smaller than that of the traditional one, therefore the accuracy of the results obtained by the proposed method is improved.

B. Multimaterial region

Figure 5 shows the analysis and display area for the multimaterial model. Here again we use the symmetry of the

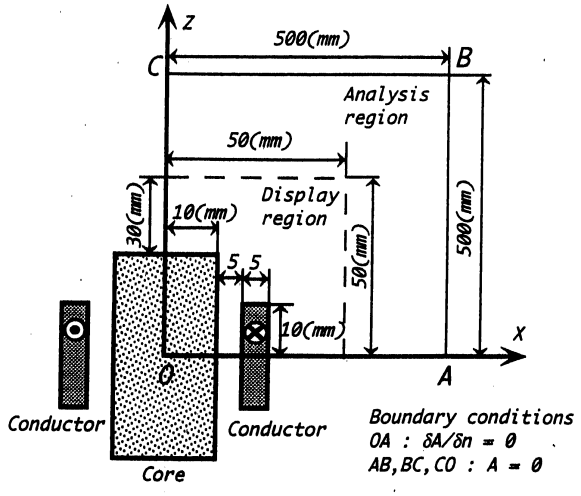

FIG. 5. Multimaterial model.

model and analyze only one quadrant. This model is quasi-3-D (a 2-D model extended into the third dimension); therefore 2-D analysis on the same model with an extremely dense finite element mesh is used as a standard value because

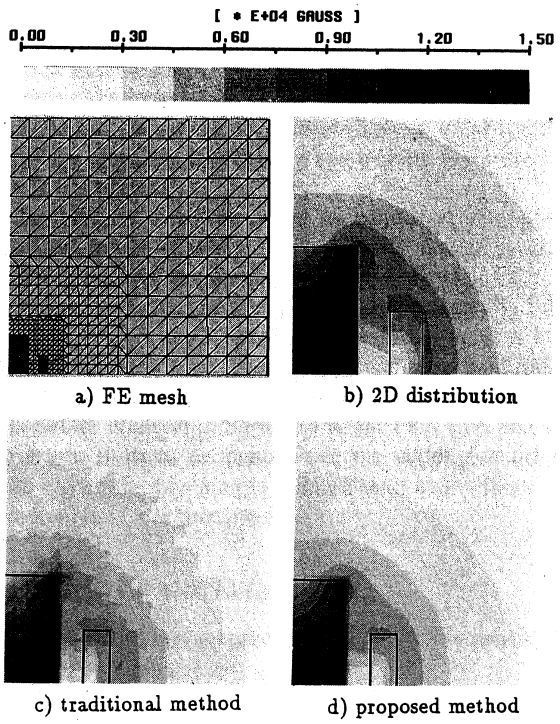

FIG. 6. Magnetic flux density distribution. (a) FE mesh, (b) 2-D distribution, (c) traditional method, and (d) proposed method.

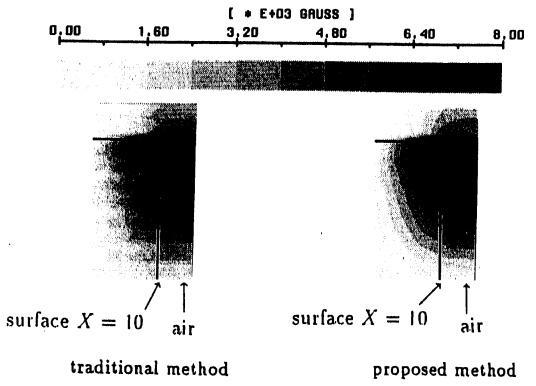

FIG. 7. The B_x distribution as a normal component on the intermaterial boundary.

no theoretical solution exists. This model is important to demonstrate the ability of our method to deal with multimaterial regions and their boundaries.

In Fig. 6, the visualization of 2-D and 3-D data using the traditional and our proposed visualization methods, again using the same scale and together with the part of interest of the finite element mesh used in the analysis are presented. It is clear that the proposed method provides a better visualization. In Fig. 7 the x component of magnetic flux density B_x as a normal component on the surface of material at $X=10$, for the traditional and the proposed visualization algorithms, is presented. The continuity of the normal components is apparent.

IV. CONCLUSION

We have presented a new, improved method for the visualization of the magnetic flux density obtained by the 3-D first-order edge FEA. The proposed method involves some algebraical averaging procedure and interpolation inside each finite element. These procedures do not have a large influence on the results of magnetic flux density vector **B**, obtained directly from the analysis, and are easily implemented and computationally efficient. Using the properties of edge FEA to satisfy only the proper boundary conditions on intermaterial boundaries, our method deals very well with them and provides smooth and highly accurate visualization. The method can be easily extended for the visualization of other magnetic quantities, such as eddy current distribution.

[1] M. L. Barton and Z. J. Cendes, J. Appl. Phys. **61**, 3919 (1987).
[2] H. Yamashita, T. Yohkoh, and E. Nakamae, IEEE Trans. Magn. **26**, 739 (1990).
[3] E. Nakamae, H. Yamashita, N. Kawano, and S. Nakano, Computer & Graphics **7**, 295 (1983).